0022-3565/07/3222-619–630$20.00
THE JOURNAL OF PHARMACOLOGY AND EXPERIMENTAL THERAPEUTICS
JPET 322:619–630, 2007

Vol. 322, No. 2
120352/3226329
Printed in U.S.A.

Pharmacological, Pharmacokinetic, and Primate Analgesic Efficacy Profile of the Novel Bradykinin B_1 Receptor Antagonist ELN441958

Jon E. Hawkinson, Balazs G. Szoke, Albert W. Garofalo, Dennis S. Hom, Hongbing Zhang, Mark Dreyer, Juri Y. Fukuda, Linda Chen, Bhushan Samant, Stellanie Simmonds,[1] Karla P. Zeitz, Angie Wadsworth, Anna Liao, Raymond A. Chavez,[2] Wes Zmolek, Lany Ruslim, Michael P. Bova, Ryan Holcomb,[3] Eduardo R. Butelman, Mei-Chuan Ko, and Annika B. Malmberg[4]

Elan Pharmaceuticals, South San Francisco, California (J.E.H., B.G.S., A.W.G., D.S.H., H.Z., M.D., J.Y.F., L.C., B.S., S.S., K.P.Z., A.W., A.L., R.A.C., W.Z., L.R., M.P.B., R.H., A.B.M.); Laboratory on the Biology of Addictive Diseases, The Rockefeller University, New York, New York (E.R.B.); and Department of Pharmacology, University of Michigan Medical School, Ann Arbor, Michigan (M.-C.K.)

Received January 23, 2007; accepted April 27, 2007

ABSTRACT

The bradykinin B_1 receptor plays a critical role in chronic pain and inflammation, although efforts to demonstrate efficacy of receptor antagonists have been hampered by species-dependent potency differences, metabolic instability, and low oral exposure of current agents. The pharmacology, pharmacokinetics, and analgesic efficacy of the novel benzamide B_1 receptor antagonist 7-chloro-2-[3-(9-pyridin-4-yl-3,9-diazaspiro[5.5]undecanecarbonyl)phenyl]-2,3-dihydro-isoindol-1-one (ELN441958) is described. ELN441958 competitively inhibited the binding of the B_1 agonist ligand [^{3}H]*des*Arg^{10}-kallidin ([^{3}H]DAKD) to IMR-90 human fibroblast membranes with high affinity (K_i = 0.26 ± 0.02 nM). ELN441958 potently antagonized DAKD (but not bradykinin)-induced calcium mobilization in IMR-90 cells, indicating that it is highly selective for B_1 over B_2 receptors. Antagonism of agonist-induced calcium responses at B_1 receptors from different species indicated that ELN441958 is selective for primate over rodent B_1 receptors with a rank order potency (K_B, nanomolar) of human (0.12 ± 0.02) ~ rhesus monkey (0.24 ± 0.01) > rat (1.5 ± 0.4) > mouse (14 ± 4). ELN441958 had good permeability and metabolic stability in vitro consistent with high oral exposure and moderate plasma half-lives in rats and rhesus monkeys. Because ELN441958 is up to 120-fold more potent at primate than at rodent B_1 receptors, it was evaluated in a primate pain model. ELN441958 dose-dependently reduced carrageenan-induced thermal hyperalgesia in a rhesus monkey tail-withdrawal model, with an ED_{50} ~3 mg/kg s.c. Naltrexone had no effect on the antihyperalgesia produced by ELN441958, indicating a lack of involvement of opioid receptors. ELN441958 is a novel small molecule bradykinin B_1 receptor antagonist exhibiting high oral bioavailability and potent systemic efficacy in rhesus monkey inflammatory pain.

This work was presented in abstract form: Hawkinson JE (2006) The novel bradykinin B_1 receptor antagonist ELN441958 is anti-hyperalgesic in two primate pain models, in the *Society for Neuroscience Abstract*; 2006 Oct 14–18; Atlanta, GA. Society for Neuroscience, Washington, DC. This work was reviewed by the Animal Care and Use Committee of The Rockefeller University, the University of Michigan, and Elan Pharmaceuticals.

[1] Current affiliation: Rinat Laboratories, Pfizer, Inc., South San Francisco, California.

[2] Current affiliation: Avigen, Inc., Alameda, California.

[3] Current affiliation: Myriad Genetics, Salt Lake City, Utah.

[4] Current affiliation: Amgen, Inc., Cambridge, Massachusetts.

Article, publication date, and citation information can be found at http://jpet.aspetjournals.org.
doi:10.1124/jpet.107.120352.

Antagonism of bradykinin receptors may prove to be a viable therapeutic strategy to reduce pain and inflammation. Initial interest focused on the constitutively expressed bradykinin B_2 receptor, which is selectively activated with high affinity by bradykinin (BK) and kallidin (KD). Recently, there has been considerable interest in the inducible B_1 receptor, which is selectively activated by *des*Arg^9-bradykinin (DABK) and *des*Arg^{10}-kallidin (DAKD), the N-terminal arginine-cleaved metabolites of BK and KD (Leeb-Lundberg et al., 2005). The B_1 receptor is not normally expressed in most

ABBREVIATIONS: BK, bradykinin; KD, kallidin; DABK, *des*Arg^9-bradykinin; DALBK, *des*Arg^9-Leu^8-bradykinin; DAKD, *des*Arg^{10}-kallidin; DALKD, *des*Arg^{10}-Leu^9-kallidin; CFA, complete Freund's adjuvant; P-gp, P-glycoprotein; CNS, central nervous system; ELN441958, 7-chloro-2-[3-(9-pyridin-4-yl-3,9-diazaspiro[5.5]undecanecarbonyl)phenyl]-2,3-dihydro-isoindol-1-one; MEM, minimum essential medium; FBS, fetal bovine serum; IL, interleukin; HBSS, Hanks' balanced salt solution; BSA, bovine serum albumin; DMSO, dimethyl sulfoxide; FLIPR, fluorometric imaging plate reader; LC/MS/MS, liquid chromatography-tandem mass spectrometry; MDCK, Madin-Darby canine kidney; MOPS, 3-(*N*-morpholino)-propanesulfonic acid; PK, pharmacokinetic; AUC, area under the concentration-time curve; DRG, dorsal root ganglion; *des*Arg^{10}HOE140, des-Arg^9-D-Arg[Hyp^3,Thi^5,D-Tic^7,Oic^8]BK; SSR240612, (2*R*)-2-[((3*R*-3-(1,3-benzodioxol-5-yl)-3-[[(6-methoxy-2-naphthyl)sulfonyl]amino]propanoyl)-amino]-3-(4-[[2*R*,6*S*)-2,6-dimethylpiperidinyl]methyl]phenyl)-*N*-isopropyl-*N*-methylpropanamide hydrochloride]; LF22-0542, *N*-[[4-(4,5-dihydro-1*H*-imidazol-2-yl)phenyl]methyl-2-[2-[[(4-methoxy-2,6-dimethylphenyl)sulfonyl]methylamino]ethoxy]-*N*-methylacetamide fumarate.

tissues, but it is dramatically up-regulated following inflammation and tissue injury, and it does not readily desensitize. The low sequence homology between B_1 and B_2 receptors (36%) is consistent with the high degree of selectivity displayed by many agonists and antagonists (Leeb-Lundberg et al., 2005).

B_1 receptors from different species fall into two pharmacological classes (Regoli et al., 2001). The rodent-like class includes rat, mouse, hamster, and dog B_1 receptors, whereas the primate-like class includes the human, rhesus, pig, and rabbit receptors. The rodent B_1 receptors are potently activated by both DABK and DAKD, whereas DAKD has considerably higher affinity for the primate receptors than does DABK. Antagonist pharmacology also differs between these two classes. For example, the prototypical B_1-receptor antagonist *des*Arg^9-Leu^8-bradykinin (DALBK) is a neutral antagonist of primate receptors, but it is a partial agonist at rodent receptors (Meini et al., 1996; MacNeil et al., 1997). In addition, several classes of small molecule B_1-receptor antagonists exhibit marked potency differences between primate and rodent receptors (Kuduk et al., 2004; Ransom et al., 2004).

It has been proposed that the B_2 receptor is involved in acute inflammation, whereas the B_1 receptor is the primary kinin receptor mediating chronic inflammation (Perkins et al., 1993). In peripheral tissues, activation of newly formed B_1 receptors promotes the generation of inflammatory mediators, including prostanoids, nitric oxide, and cytokines, resulting in plasma extravasation, leukocyte trafficking, edema, and pain (McLean et al., 2000; Eisenbarth et al., 2004; Lawson et al., 2005; Leeb-Lundberg et al., 2005). B_1 receptors are constitutively expressed on primary afferent pain fibers, and they are up-regulated following nerve injury (Levy and Zochodne, 2000). Activation of neuronal B_1 receptors may contribute to neuropeptide release and subsequent neurogenic inflammation in peripheral tissues (McLean et al., 2000) as well as central sensitization at the level of the spinal cord (Pesquero et al., 2000). B_1 agonists injected dermally produce pain in humans, which is exacerbated by prior ultraviolet irradiation of the injection area (Eisenbarth et al., 2004).

B_1 receptor knockout mice have a pain phenotype implicating a role for this receptor in inflammatory and neuropathic pain. These B_1 receptor-deficient mice exhibit reduced responding in several experimental pain models relative to wild-type mice, including acute tests (hot-plate and tail-flick), following formalin, capsaicin, or complete Freund's adjuvant (CFA) injection into the paw, and in the partial sciatic nerve ligation model of neuropathic pain (Pesquero et al., 2000; Ferreira at el., 2001; Porreca et al., 2006).

Peptide antagonists including DALBK and *des*Arg^{10}HOE140 provided early pharmacological evidence in rodents implicating the role of the B_1 receptor in pain. Peptide antagonists are effective in early and late-phase licking following formalin injection into the paw (Ferreira et al., 2002), CFA-induced thermal and mechanical hyperalgesia (Fox et al., 2003), and carrageenan-induced mechanical hyperalgesia (Poole et al., 1999). Peptide antagonists also reduce thermal and mechanical hyperalgesia in models of neuropathic pain, e.g., in the rat chronic constriction nerve injury model (Levy and Zochodne, 2000).

More recently, small molecule B_1 receptor antagonists have shown efficacy in rodent pain models. SSR240612 reduced late-phase licking in the mouse formalin model, inhibited thermal hyperalgesia induced by ultraviolet irradiation in rats and also reduced thermal hyperalgesia in the rat chronic constriction nerve injury nerve injury model (Gougat et al., 2004). LF22-0542 reduced responding in the late phase of the formalin model and in the acetic acid-induced writhing model in mice, and it also reduced formalin-induced flinching, carrageenan-induced mechanical hyperalgesia, and CFA-induced thermal hyperalgesia in rats (Porreca et al., 2006). LF22-0542 reduced thermal, but not mechanical, hyperalgesia in the rat spinal nerve ligation model (Porreca et al., 2006).

In the present study, we describe the in vitro pharmacological profile, metabolic stability, P-glycoprotein (P-gp) liability, CNS penetration, in vivo pharmacokinetics, and primate analgesic efficacy of the novel B_1 receptor antagonist ELN441958 (Fig. 1).

Materials and Methods

Synthesis of ELN441958. Addition of *tert*-butyl 3,9-diazaspiro[5.5]undecane-3-carboxylate to 4-chloropyridine hydrochloride followed by deprotection in neat trifluoroacetic acid affords 3-(4-pyridinyl)-3,9-diazaspiro[5.5]undecane trifluoroacetate. Addition of methyl 3-aminobenzoate to methyl 2-(bromomethyl)-6-chlorobenzoate followed by ester hydrolysis gives 3-(7-chloro-1-oxo-1,3-dihydroisoindol-2-yl)benzoic acid, which is then coupled with 3-(4-pyridinyl)-3,9-diazaspiro[5.5]undecane trifluoroacetate to afford 7-chloro-2-[3-(9-pyridin-4-yl-3,9-diazaspiro[5.5]undecanecarbonyl) phenyl]-2,3-dihydro-isoindol-1-one (ELN441958).

Recombinant Cell Lines. The complete open reading frame encoding the bradykinin B_1 receptor (BKB1R) is contained within a single exon in both the mouse and rat genomes. Accordingly, the cDNAs for each BKB1R were amplified from mouse and rat genomic DNA (Clontech, Mountain View, CA) using primers specific for the 5′ and 3′ ends of the respective coding regions (GenBank, mouse: U47281; rat: U66107). Polymerase chain reaction amplification was achieved under standard conditions, using a combination of *Taq* and *Pfu* DNA polymerases for improved fidelity. Amplification products were subcloned into the TOPO TA cloning vector pCR 2.1 TOPO (Invitrogen, Carlsbad, CA) and sequenced. The correct BKB1R cDNA was subcloned out of the TOPO TA vector and introduced into a pEAK 8 plasmid (Edge Biosystems, Gaithersburg, MD) that was previously modified by the addition of novel sites in the polylinker region by an overlapping oligonucleotide strategy. This plasmid is an episomal vector that drives transgene expression with the eF1α promoter, and stable clones can be selected with puromycin. The mouse and rat BKB1R pEAK plasmids were stably transfected into PEAK-R and PEAK-S cells (Edge Biosystems), modified human embryonic kidney 293 cells designed specifically to preserve episomal vector expression. Stable populations of cells were maintained with puromycin. Stable transfectants of either PEAK-R or PEAK-S cells were selected based on their responsiveness in the cell-based assay (see below).

Cell Culture. IMR-90 human lung fibroblast cells (CCL-186; American Type Culture Collection, Manassas, VA) and DBS-FRhL-2 rhesus lung fibroblast cells (CL-160; American Type Culture Collection) were grown in Eagle's minimum essential medium (MEM) supplemented with 10% fetal bovine serum (FBS) as recommended

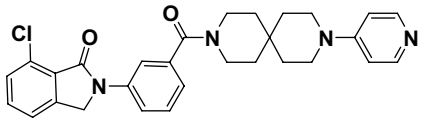

Fig. 1. Structure of ELN441958.

by American Type Culture Collection. Peak-S or -R cells expressing recombinant rat or mouse B_1 receptors, respectively, were cultured in Dulbecco's modified Eagle's medium supplemented with 10% FBS, 400 μg/ml hygromycin B, and 1.5 μg/ml puromycin.

Radioligand Binding. Confluent IMR-90 cells were treated with 0.35 ng/ml interleukin (IL)-1β in 10% FBS/MEM for 4 h to up-regulate B_1 receptors. Cells were then rinsed with phosphate-buffered saline, collected by scraping in ice-cold TES buffer (25 mM NaTES, 1 mM phenantroline, 2 μM captopril, and 140 μg/ml bacitracin, pH 7.4), and centrifuged at 3200*g* for 5 min. Pellets were homogenized in TES buffer on ice using a polytron-type homogenizer (VirTis, Gardiner, NY). The membranes were collected and washed by centrifugation twice at 50,000*g* for 20 min at 4°C. Pellets were resuspended in buffer at 0.5 mg/ml protein and stored at −80°C. Protein concentration was measured using the bicinchoninic acid method in the presence of 2% SDS (Pierce Chemical, Rockford, IL). Displacement binding experiments were carried out in 96-deep well plates in binding buffer [20 mM HEPES in Hanks' balanced salt solution (HBSS) without bicarbonate or phenol red, 0.1% BSA, 1 mM phenantroline, 2 μM captopril, and 140 μg/ml bacitracin, pH 7.4] at room temperature. Approximately 40 μg of membranes/well were incubated with ~0.5 nM [^{3}H]DAKD (PerkinElmer Life and Analytical Sciences, Wellesley, MA) in the absence or presence of different concentrations of test compounds in a final volume of 300 μl. The actual [^{3}H]DAKD concentration used in each experiment was determined by sampling the working solution of [^{3}H]DAKD in binding buffer and counting on a scintillation counter (LS5000; Beckman Coulter, Fullerton, CA). Test compounds were diluted in seven half-log steps at 100× final concentration in DMSO, and then they were assayed in duplicate wells (final 1% DMSO). Nonspecific binding was determined in the presence of 1 μM DAKD. After a 1-h incubation, binding was terminated by rapid filtration through GF/B filter plates (Whatman, Florham Park, NJ) presoaked in 0.2% polyethyleneimine using a Packard Filtermate (PerkinElmer Life and Analytical Sciences). Filters were rinsed four times with ice-cold wash buffer (50 mM Tris-HCl, pH 7.4), and bound radioactivity was counted after the addition of a scintillant in a MicroBeta scintillation counter (PerkinElmer Life and Analytical Sciences). Following correction for nonspecific binding, IC_{50} values were calculated using the four-parameter sigmoidal concentration-response function, and K_D and B_{max} values were calculated using the hyperbolic function (Prism; GraphPad Software Inc., San Diego, CA). Binding K_i values were calculated according to the Cheng-Prusoff equation using the K_D of [^{3}H]DAKD (0.31 nM) determined in saturation binding experiments.

Calcium Mobilization (FLIPR). Human (IMR-90) and rhesus (DBS-FRhL-2) lung fibroblast cells expressing native B_1 receptors were harvested by trypsinization and seeded into black wall/clear bottom 96-well plates (Costar 3904; Corning Life Sciences, Acton, MA) at approximately 13,000 cells/well. The following day, cells were treated with 0.35 ng/ml human IL-1β in 10% FBS/MEM for 2 h to up-regulate B_1 receptors. Induced cells were loaded with fluorescent calcium indicator by incubation with 2.3 μM Fluo-4/acetoxymethyl ester (Invitrogen) at 37°C for 1.5 h in the presence of an anion transport inhibitor (2.5 mM probenecid in 1% FBS/MEM). Extracellular dye was removed by washing with assay buffer (2.5 mM probenecid and 0.1% BSA in 20 mM HEPES/HBSS without bicarbonate or phenol red, pH 7.5), and cell plates were kept in the dark until used. Test compounds were assayed at seven concentrations in triplicate. Addition of test compounds to the cell plate and incubation for 5 min at 35°C, followed by the addition of 2 to 8 nM final ($3 \times EC_{50}$) B_1 agonist DAKD (Bachem California, Torrance, CA), were carried out in the fluorometric imaging plate reader (FLIPR; Molecular Devices, Sunnyvale, CA) while continuously monitoring calcium-dependent fluorescence. B_2 responses were measured in IMR-90 cells in an identical manner except that the IL-1β treatment step was omitted and BK (0.7 nM final; $3 \times EC_{50}$) replaced DAKD as agonist. Cells expressing recombinant rat or mouse B_1 receptors were detached using PBS without calcium or magnesium and loaded with 3.6 μM Fluo-4/acetoxymethyl ester for 75 min at 37°C in 1% FBS-containing HEPES/HBSS without bicarbonate or phenol red, pH 7.5. Loaded cells were washed by centrifugation, resuspended in assay buffer (0.1% BSA in HEPES/HBSS solution), and plated into 96-well black/clear plates at 100,000 cells/well. Plates were centrifuged (200*g*; 10 min) to move cells to the bottom of wells, and then they were assayed in the FLIPR as described above, with DABK as agonist at $3 \times EC_{50}$ concentration (4–10 nM). Peak height of agonist-induced fluorescence as a function of antagonist concentration was fitted to the sigmoidal function (Prism; GraphPad Software Inc.) to determine IC_{50} values. K_B values were calculated according to the Cheng-Prusoff equation using the EC_{50} of the agonist used for each species of receptor (Table 2).

Solubility. ELN441958 was dissolved in DMSO as a 20 mM stock solution, diluted 200-fold in HBSS, pH 7.4, shaken overnight at room temperature, and centrifuged at 14,000*g* for 60 min. The concentration of ELN441958 in the supernatant was determined using high-performance liquid chromatography-UV (aqueous acetonitrile containing 0.1% formic acid mobile phase) by comparing its peak area to a standard curve.

Metabolic Stability. ELN441958 (1 μM) was incubated at 37°C with rat or human liver microsomes (0.5 mg/ml; BD Biosciences, Bedford, MA) in the presence of 1 mM NADPH for 60 min. Aliquots were taken at 0, 5, 12, 20, 30, 45, and 60 min, precipitated with organic solvent containing internal standard, and analyzed by LC/MS/MS using a C18 column (2.1 × 50 mm, 5 μm; Sepax GPC18; Sepax Technologies, Newark, DE; flow 900 μl/min) with aqueous acetonitrile containing 0.1% formic acid as mobile phase. The amount of parent compound remaining at each time point was estimated by the chromatographic peak area ratios and then plotted using a log-linear fit to determine the first-order rate constant. Midazolam, a high-clearance positive control, was incubated in parallel in each experiment.

Permeability. ELN441958 was evaluated for its permeability across a monolayer of Madin-Darby canine kidney (MDCK) II cells (American Type Culture Collection). Cells were grown for 4 days in Dulbecco's modified Eagle's medium with GlutaMAX containing 10% heat-inactivated FBS and 40 units/ml penicillin/streptomycin at 37°C and 5% CO_2, and they were plated into 12-mm-diameter 12-well Transwell plates (Corning Life Sciences). ELN441958 (5 μM) was added in HEPES/HBSS with 0.1% glucose, pH 7.4, and plates were incubated for 2 h at 37°C with shaking. Donor and receiver wells were then sampled and assayed by LC/MS/MS to determine compound levels. From these data, the forward flux (apical to basolateral) was calculated. The extent of transport by P-gp was determined in the same manner, except that MDCK cells expressing human multidrug resistance (MDR)-1 (kind gift from Dr. Piet Borst, The Netherlands Cancer Institute, Amsterdam, The Netherlands) were used, and the forward flux was calculated in the absence or presence of the P-gp inhibitor cyclosporine A at 10 μM (Sigma-Aldrich, St. Louis, MO). The known P-gp substrate indinavir was used a positive control. Integrity of the monolayer was determined using 100 μM lucifer yellow (Sigma-Aldrich) with <2% leakage observed in all experiments.

ATPase. Membranes prepared from Sf9 insect cells expressing human MDR1 using the baculovirus expression system (*Autographa californica*) were purchased from BD Biosciences. The ATPase reaction was carried out in a 35-μl reaction volume in a 384-well microtiter plate containing 1% DMSO, 0.1 to 100 μM ELN441958, and 0.67 mg/ml Sf9 membranes in a reaction buffer consisting of 50 mM KCl, 50 mM MOPS-Tris, pH 7.0, with 5 mM sodium azide, 2 mM dithiothreitol, 0.1 mM EGTA, and 1 mM ouabain. The reaction was started with the addition of MgATP (5 mM final), incubated for 50 min at 37°C, and then quenched with SDS (2.2% final). The colorimetric reaction was developed for 40 min at 37°C following addition of the detection reagent consisting of 60 mM ammonium molybdate and 15 mM zinc acetate, and then the absorbance was determined at

800 nm using a Safire[2] microplate reader (Tecan, Durham, NC). Indinavir was used as a positive control.

ELN441958 Formulation. To achieve maximal exposure for pharmacokinetic and efficacy studies, ELN441958 was formulated as a clear solution. For rodent studies, ELN441958 was dissolved in 2% Tween 80 in saline and adjusted to pH 4.5 to 7 with HCl. For rhesus PK studies, ELN441958 was formulated in 10% polyethylene glycol 660 hydroxystearate (Solutol; BASF, Ludwigshafen, Germany) in either saline (i.v.) or water (p.o.), adjusted to pH 4.5 to 7 with HCl. For s.c. administration in rhesus monkeys in both PK and efficacy studies, it was formulated as a clear solution in 20% Captisol (sulfobutylether-β-cyclodextrin; CyDex, Lenexa, KS) in water adjusted to pH 4.5 to 7 with formic acid.

Pharmacokinetic Analysis. Aliquots of plasma (100 μl) from rhesus monkeys or Sprague-Dawley rats were added to extraction plates containing an internal standard in 400 μl of methanol/acetonitrile (50:50) and mixed. After centrifugation, the supernatant was transferred to a 96-deep well plate and evaporated to dryness. The residue was reconstituted in 20% methanol/0.1% formic acid mobile phase, and it was analyzed by LC/MS/MS using a C18 column and an API-3000 triple quadrupole mass spectrometer (Applied Biosystems, Foster City, CA). Plasma concentrations were determined from a calibration curve prepared by extracting known amounts of ELN441958 from control plasma. The sensitivity limit was approximately 0.25 ng/ml or ng/g ELN441958 per sample.

Mouse CNS Penetration. To assess the contribution of P-gp to CNS penetration, the brain and plasma levels of ELN441958 in female FVB wild-type mice were compared with MDR1 a/b (−/−) knockout mice (Taconic Farms, Germantown, NY) at 5 min following a single 2.5 mg/kg i.v. bolus injection. To assess the time course of CNS penetration, brain, spinal cord, and plasma levels were measured in male FVB wild-type mice at 0.5, 1, 2, and 4 h following s.c. administration of 10 mg/kg ELN441958. LC/MS/MS quantitation and tissue sample preparation were as described above, except that ELN441958 levels in brain and spinal cord were quantitated following homogenization of the preweighed tissue in ethyl acetate, and calibration curves were prepared by extracting known amounts of ELN441958 from ethyl acetate homogenates of control tissue. Mouse tissues were perfused, and the reported brain concentration was adjusted for the concentration of ELN441958 in plasma. The total area under the concentration-time curve from time 0 to 4 h ($AUC_{0\text{-}4\ h}$) was estimated from plasma, brain, and spinal cord concentrations using standard methods. These values were then used to calculate brain/plasma and spinal cord/plasma ratios.

Carrageenan-Induced Hyperalgesia. Adult male and female rhesus monkeys (*Macaca mulatta*) (weight range 8–11 kg; $n = 3$) were trained in the tail-withdrawal procedure described by Ko and Lee (2002). A 20-s maximal tail-withdrawal latency (baseline cut-off) was used with a normally non-noxious thermal stimulus of 46°C. To produce inflammation-associated hyperalgesia, carrageenan (2 mg/tail in 0.1 ml of saline s.c.) was injected into the terminal 1 to 4 cm of the tail, and tail-withdrawal latencies were measured every 30 min for 3.5 h. ELN441958 (1, 3, or 10 mg/kg) or naproxen (10 mg/kg) was injected s.c. on the back 30 min before carrageenan injection. In the opioid-receptor antagonist study, 1 mg/kg naltrexone s.c. was administered on the back just before ELN441958. Blood samples for compound analysis were drawn 4 h after carrageenan injection (4.5 h after the ELN441958 administration).

Results

Potency and Selectivity of ELN441958 at Bradykinin B_1 Receptors. ELN441958 inhibited the binding of the agonist radioligand [^{3}H]DAKD to the human B_1 receptor present in IMR-90 lung fibroblast cell membranes with high affinity ($K_i = 0.26 \pm 0.02$ nM) (Fig. 2; Table 1). The peptide antagonist DALKD had a similar subnanomolar affinity,

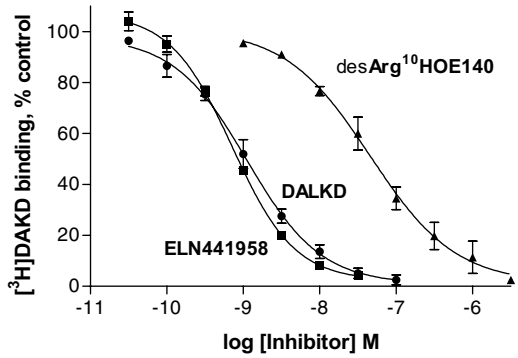

Fig. 2. ELN441958 is a subnanomolar inhibitor of [^{3}H]DAKD binding to the native human bradykinin B_1 receptor. Inhibition of radioligand binding to membranes prepared from IMR-90 human lung fibroblasts. See Table 1 for K_i values.

TABLE 1
Affinity of ELN441958 and peptidic antagonists for the native human bradykinin B_1 receptor
Inhibition of radioligand binding to membranes prepared from IMR-90 human lung fibroblasts. See Fig. 2 for displacement curves. Data are means ± S.E.M. of at least three experiments.

Antagonist	K_i	Hill Slope
	nM	
ELN441958	0.26 ± 0.02	1.1 ± 0.1
DALKD	0.49 ± 0.06	0.98 ± 0.06
*des*Arg^{10}HOE140	15 ± 3	0.88 ± 0.07

whereas *des*Arg^{10}HOE140 had more than 50-fold lower affinity. Saturation binding studies were performed to determine the type of inhibition (Fig. 3). K_D and B_{max} values (mean ± S.E.M.; $n = 3$) were 0.31 ± 0.03 nM and 1.8 ± 0.5 pmol/mg, respectively, in the control condition. In the presence of 0.5 nM ELN441958, K_D and B_{max} values were 1.3 ± 0.1 nM and 1.7 ± 0.4 pmol/mg, respectively, consistent with competitive inhibition.

ELN441958 is a potent, neutral antagonist of B_1 receptor activation based on the inhibition of agonist-induced increases in intracellular calcium in native and recombinant cells. The potencies for stimulation of calcium mobilization by the appropriate agonist for B_1 receptors from the different species examined, i.e., DAKD at the human and rhesus monkey B_1 receptors and DABK at rat and mouse B_1 receptors, are shown in Table 2. In IMR-90 cells expressing the native human B_1 receptor, ELN441958 produced a concentration-dependent antagonism of the DAKD-induced calcium mobilization with a K_B of 0.12 ± 0.02 nM (Figs. 4A and 5A; Table 3). ELN441958 itself does not produce an agonist response at concentrations completely blocking the agonist-induced response at all four species of receptor tested, indicating that it is a neutral antagonist in this assay (data for the rat receptor is shown in Fig. 4B). In contrast, the peptide antagonist DALKD exhibits clear agonism at rodent B_1 receptors (Fig. 4B) as reported previously (Meini et al., 1996; MacNeil et al., 1997). A very small agonist response was generally observed following application of *des*Arg^{10}HOE140 at high concentrations. The rank order potency for ELN441958 antagonism of B_1 receptors from different species was human ~ rhesus > rat > mouse; it was 120-fold less potent at the mouse relative to human receptor (Fig. 5; Table 3). In contrast, the peptide antagonists showed much less species difference in antagonist potency. The rank order potency for DALKD antagonism

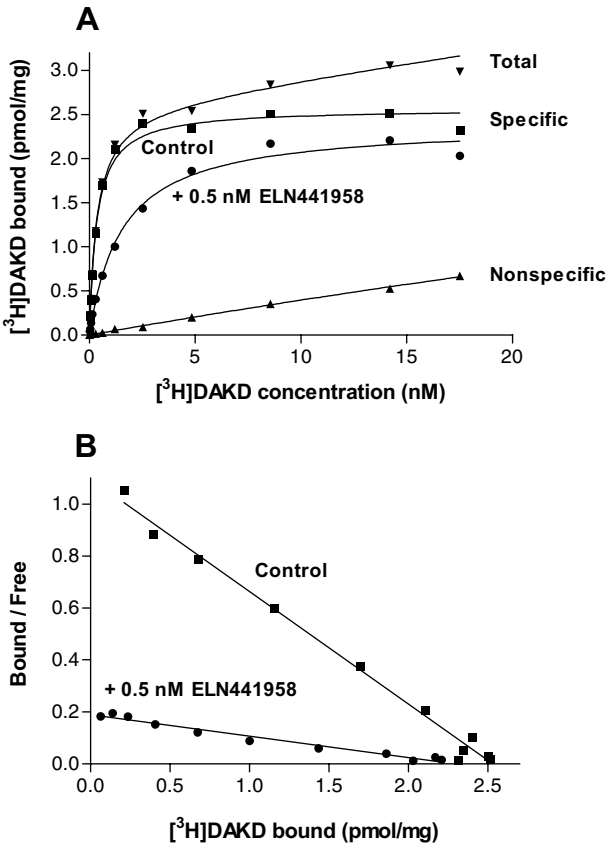

Fig. 3. ELN441958 competitively displaces the selective B_1-receptor peptide agonist ligand [^{3}H]DAKD from the native human B_1 receptor. A, representative [^{3}H]DAKD saturation experiment in IMR-90 cell membranes. Specific binding in the absence (control) and presence of 0.5 nM ELN441958 were calculated by subtraction of the linear regression of the nonspecific binding (determined in the presence of 1 μM DAKD) from the total binding. Total binding shown is from the control condition. Data points represent averages of duplicates. B, Scatchard transformation of the specific binding data from Fig. 3A. In this experiment, K_D and B_{max} values were 0.36 nM and 2.6 pmol/mg, respectively, in the control condition and 1.6 nM and 2.4 pmol/mg, respectively, in the presence of ELN441958.

TABLE 2

Agonist potency for mobilization of intracellular calcium at rodent and primate bradykinin B_1 receptors

Potencies for stimulation of calcium mobilization measured using the FLIPR using DAKD as agonist in lung fibroblasts cell lines expressing native B_1 receptors from human (IMR-90) and rhesus monkey (DBS-FRhL-2) or using DABK as agonist in HEK293 cells expressing recombinant rat and mouse B_1 receptors. Data are means ± S.E.M. of at least four to five experiments.

Species	Agonist[a]	EC_{50}	Hill Slope
		nM	
Human	DAKD	0.88 ± 0.14	1.1 ± 0.1
Rhesus	DAKD	0.83 ± 0.10	0.85 ± 0.07
Rat	DABK	3.0 ± 0.4	1.0 ± 0.1
Mouse	DABK	1.7 ± 0.3	1.1 ± 0.1

[a] Receptors were activated using the probable physiologic agonist. For reference, the EC_{50} values for activation of human and rhesus B_1 receptors by DABK were 118 and 34 nM, respectively, and for rat and mouse B_1 receptors by DAKD were 2.6 and 2.2 nM, respectively (n = 1–4).

of B_1 receptors was rhesus ~ human > mouse ~ rat, with a 7-fold difference between rhesus and rat receptors. The less potent antagonist *des*Arg^{10}HOE140 showed very little species difference, a range of only 4-fold across the four species.

ELN441958 is highly selective for B_1 over B_2 receptors. In IMR-90 cells, ELN441958 failed to inhibit the calcium mobilization induced by the selective B_2-receptor agonist BK at concentrations up to 10 μM (data not shown). Likewise, *des*Arg^{10}HOE140 and DALKD were inactive at inhibit-

TABLE 3

Potency of ELN441958 and peptidic antagonists for inhibition of agonist-induced calcium mobilization at rodent and primate bradykinin B_1 receptors

Inhibition of DAKD (human and rhesus) or DABK (rat and mouse)-stimulated calcium mobilization in cells expressing native (human and rhesus) or recombinant (rat and mouse) B_1 receptors. See Fig. 5 for concentration-response curves. Data are means ± S.E.M. of at least three experiments

Antagonist	Species	K_B	Hill Slope
		nM	
ELN441958	Human	0.12 ± 0.02	1.12 ± 0.04
	Rhesus	0.24 ± 0.01	0.67 ± 0.07
	Rat	1.5 ± 0.4	1.4 ± 0.2
	Mouse	14 ± 4	1.6 ± 0.2
DALKD	Human	0.28 ± 0.02	1.7 ± 0.5
	Rhesus	0.17 ± 0.01	1.5 ± 0.3
	Rat	1.9 ± 0.2	1.1 ± 0.1
	Mouse	1.1 ± 0.1	1.4 ± 0.2
*des*Arg^{10}HOE140	Human	22 ± 3	0.77 ± 0.06
	Rhesus	5.3 ± 1.1	0.85 ± 0.10
	Rat	11 ± 2	1.4 ± 0.2
	Mouse	5.4 ± 1.0	2.0 ± 0.2

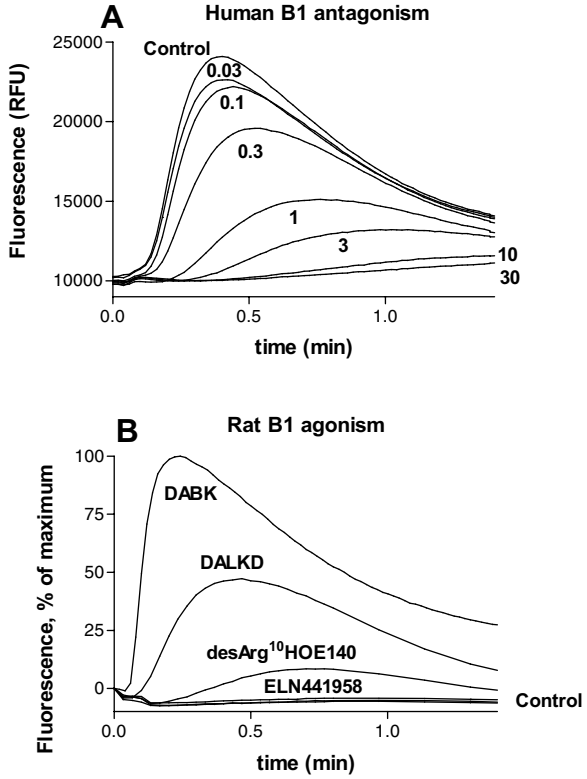

Fig. 4. ELN441958 is a neutral antagonist of B_1 agonist-induced calcium mobilization. Traces represent changes of Fluo-4 fluorescence in cells expressing B_1 receptors measured using FLIPR. A, concentration-dependent antagonism of DAKD-induced calcium release by 0.03 to 30 nM ELN441958 at the native human receptor present in IMR-90 cells. K_B and Hill slope values for this experiment were 0.17 nM and 0.86, respectively. B, partial agonism of DALKD and *des*Arg^{10}HOE140, but not ELN441958, at the recombinant rat B_1 receptor. Traces shown are from a single representative experiment. In this experiment, 300 nM DALKD and 3 μM *des*Arg^{10}HOE140 exhibited calcium-related fluorescent peak responses of 54 and 14%, respectively, relative to the full agonist DABK at 300 nM. DALKD and *des*Arg^{10}HOE140 agonism ranged from 20 to 55% (n = 3) and from <1 to 19% (n = 7), respectively, relative to 300 nM DABK. Responses to ELN441958 up to 300 nM were indistinguishable from that of control in all experiments (n = 4).

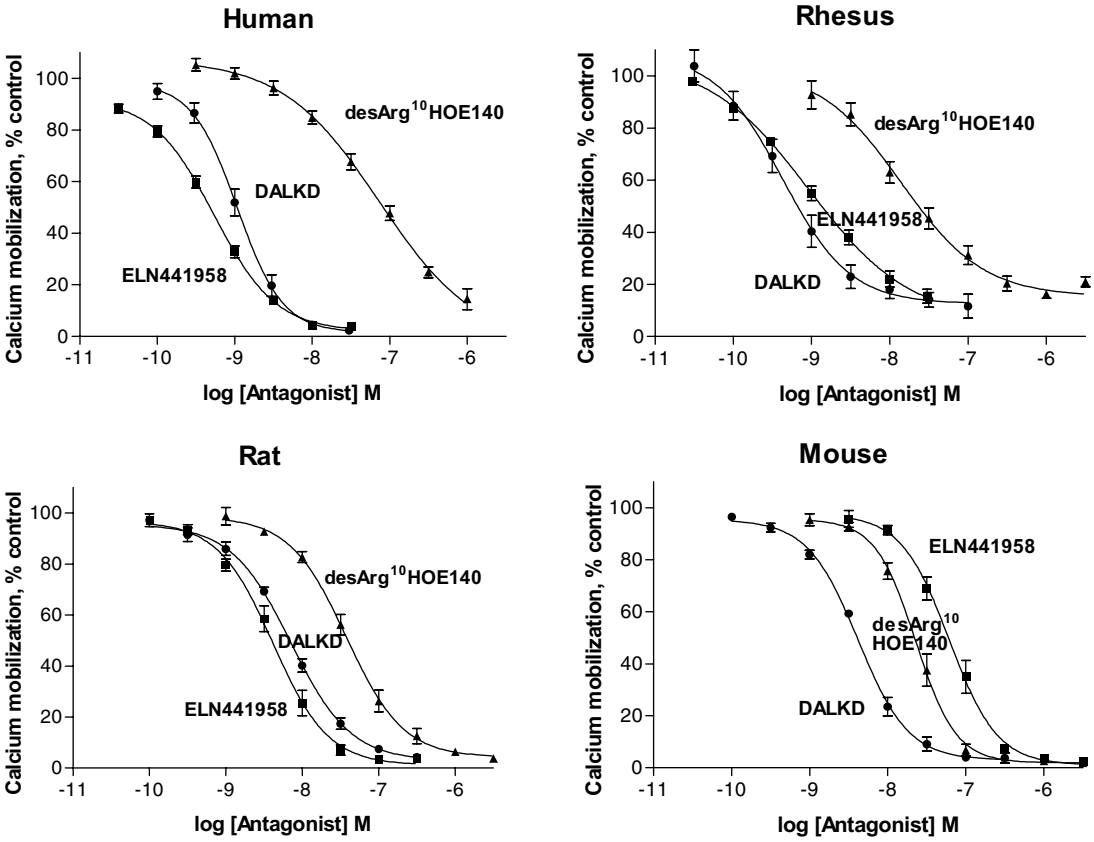

Fig. 5. ELN441958 exhibits species differences in potency for antagonism of selective B_1 agonist-induced calcium mobilization. Antagonism of DAKD (human and rhesus) or DABK (rat and mouse)-induced calcium increase in cells expressing either native (human and rhesus) or recombinant (rat and mouse) B_1 receptors indicated by Fluo-4 fluorescence using FLIPR. Means ± S.E.M. of at least three experiments. Calculated K_B values are shown in Table 3.

ing BK-induced responses up to 5 and 30 μM, respectively. In contrast, the selective B_2 receptor antagonist HOE140 potently inhibited the BK-induced response (IC_{50} = 2.3 ± 0.4 nM). Regarding other nontarget receptors, 10 μM ELN441958 produced ≥50% inhibition at 20 of more than 100 enzyme and receptor assays tested in a broad panel (data not shown). Of these, IC_{50} values were determined for five receptors in single experiments. The most potent off-target activity identified was at the human μ-opioid receptor (binding K_i = 0.13 μM), suggesting >500-fold selectivity for B_1 over μ-opioid receptors. Lower potency inhibition was measured at the human muscarinic M1, δ-opioid, and κ-opioid receptors (binding K_i values of 0.37, 0.69, and 1.5 μM). Because in vivo analgesia studies could be complicated by agonism at opioid receptors, ELN441958 was tested in guanosine 5′-*O*-(3-[^{35}S]thio)triphosphate binding assays and found to be an agonist at the δ-opioid receptor (EC_{50} = 0.76 μM) and also exhibited weak agonism at the μ-opioid receptor (<50% stimulation at 10 μM) (data not shown).

Metabolic Stability, Permeability, P-Glycoprotein Liability, and CNS Penetration. ELN441958 was sufficiently soluble (69 ± 16 μM) in aqueous buffer at pH 7.4 for further characterization of metabolic stability and permeability. ELN441958 demonstrated good metabolic stability with low in vitro intrinsic clearance in rat, rhesus, and human microsomes (Table 4). In contrast, the metabolically labile positive control midazolam was cleared much more rapidly. ELN441958 had moderate permeability in MDCK II cells (Table 5). However, the permeability of ELN441958 in MDCK cells expressing the recombinant human MDR1 gene coding for P-gp (MDR1-MDCK cells) was substantially lower. Cyclosporine A, an inhibitor of P-gp, increased the permeability in these cells 13-fold. The known P-gp substrate indinavir exhibited similar behavior in these assays, but it had substantially lower intrinsic permeability than ELN441958. In addition, ELN441958 stimulated P-gp ATPase activity 2-fold in membranes expressing the recombinant human MDR1 gene. Taken together, these data indicate that ELN441958 is a substrate for P-gp.

P-gp is one of the components of the blood-brain barrier,

TABLE 4
ELN441958 has good in vitro metabolic stability across species
Metabolic clearance determined by decay of parent compound incubated with microsomes as measured by LC/MS/MS. Data are means ± S.E.M. (n = 4).

Compound	Rat	Rhesus	Human
ELN441958			
$t_{1/2}$ (min)	50 ± 2	43 ± 4	48 ± 3
Intrinsic clearance (μl/mg/min)	28 ± 1	33 ± 3	29 ± 2
Midazolam			
$t_{1/2}$ (min)	1.6 ± 0.4	3.3 ± 1.3	3.7 ± 0.8
Intrinsic clearance (μl/mg/min)	1200 ± 400	650 ± 230	430 ± 100

TABLE 5
ELN441958 is a substrate for P-glycoprotein
See *Materials and Methods* for description of the assays. Values are means ± S.E.M. of at least three independent in vitro experiments or single in vivo studies (n = 3–4).

Assay or Model	ELN441958	Indinavir
P-gp ATPase (-fold stimulation over basal)	2.1 ± 0.2	7.1 ± 0.9
P-gp ATPase EC_{50} (nM)	N.A.[a]	1.5 ± 0.1
MDCK II permeability[b] (nm/s)	54 ± 8	24 ± 4
MDR1-MDCK permeability[c] (nm/s)	7.8 ± 2.0	3.1 ± 0.3
MDR1-MDCK permeability + cyclosporine A (nm/s)	110 ± 50	27 ± 7
Cyclosporine A permeability ratio	13 ± 3	9 ± 3
Brain level in wild-type FVB mouse[d] (μM)	<0.002	0.042 ± 0.008
Brain level in MDR1 a/b (−/−) mouse[e] (μM)	1.5 ± 0.3	0.40 ± 0.03

[a] Stimulation produced by ELN441958 was too low to calculate an EC_{50} value.
[b] Percentage of recoveries for ELN441958 and indinavir were 44 ± 5 and 82 ± 3, respectively.
[c] Percent recoveries for ELN441958 and indinavir were 41 ± 4 and 59 ± 16, respectively.
[d] Plasma levels for ELN441958 and indinavir were 7.4 ± 0.5 and 3.2 ± 0.1 μM, respectively.
[e] Plasma levels for ELN441958 and indinavir were 20.0 ± 0.3 and 3.8 ± 0.1 μM, respectively.

and it is known to limit CNS penetration of certain compounds (Demeule at al., 2002). Because in vitro assays predicted that the CNS exposure of ELN441958 may be limited by P-gp, an in vivo study comparing brain levels in wild-type mice to MDR1 knockout mice was done. Five minutes after an i.v. dose of 2.5 mg/kg, ELN441958 achieved low micromolar brain levels in MDR1 knockout mice, but it was below the limit of quantitation in wild-type mice (Table 5), consistent with P-gp-mediated extrusion from the CNS. To further characterize the CNS penetration by this compound, a brain and spinal cord time-course study was performed in wild-type mice. As shown in Fig. 6, the levels of ELN441958 were considerably lower in brain and spinal cord relative to plasma at all of the time points measured. Based on the AUC ratios, ELN441958 exposure in the spinal cord and brain was 1.4 and 6.7%, respectively, of plasma exposure (Table 6).

Pharmacokinetics. ELN441958 exhibits a favorable pharmacokinetic profile in the rat (Fig. 7; Table 7). After an i.v. dose of 2.5 mg/kg, ELN441958 had a moderate volume of distribution (2.7 l/kg, approximately four times total body water) and a moderate clearance (0.96 l/h/kg, approximately 24% of hepatic blood flow). The terminal plasma half-life of this compound in rats was 1.7 h. When dosed orally, concentrations of ELN441958 increased to a maximum of 1.2 μg/ml at 2 h after dosing. The oral availability of ELN441958 in rats was 57%.

ELN441958 had an excellent pharmacokinetic profile in rhesus monkeys (Fig. 8; Table 7). When dosed i.v. at 1 mg/kg, ELN441958 had a moderate volume of distribution (2.7 l/kg) and a moderate clearance (0.49 l/h/kg, approximately 32% of hepatic blood flow). The terminal plasma half-life of this compound was 3.9 h in rhesus monkeys. After oral dosing, concentrations of ELN441958 increased to a maximum of 3.6 μg/ml at 3.3 h after dosing. The calculated oral bioavailability was greater than 100%. The pharmacokinetics of ELN441958 was also examined in rhesus monkeys by the s.c. route of administration to support efficacy studies. At an s.c. dose of 10 mg/kg, ELN441958 achieved peak plasma levels of 5.6 μg/ml at 2.2 h postdose. The calculated s.c. bioavailability was also greater than 100%.

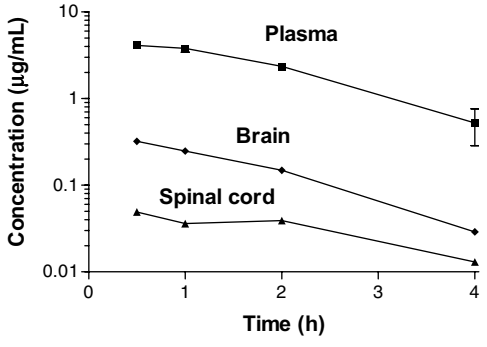

Fig. 6. ELN441958 CNS exposure correlates with plasma levels in the mouse. ELN441958 was administered at 10 mg/kg s.c. (n = 3). Tissue levels were determined by LC/MS/MS.

TABLE 6
ELN441958 has low CNS exposure in the mouse
See Fig. 6 and *Materials and Methods* for experimental details.

Tissue	C_{max}	$AUC_{0-4\ h}$	Plasma Ratio
	μg/ml	μg · h/ml	
Plasma	4.1 ± 0.2	8.9 ± 0.7	1.0
Brain	0.32 ± 0.16	0.60 ± 0.12	0.067
Spinal cord	0.049 ± 0.02	0.12 ± 0.02	0.014

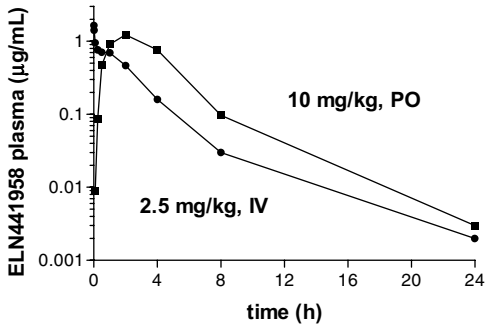

Fig. 7. ELN441958 exhibits a favorable pharmacokinetic profile in the rat. Rats were dosed i.v. or orally with ELN441958 in 2% Tween 80/saline at 2.5 or 10 mg/kg, respectively (n = 3). See *Materials and Methods* for analytical details.

Carrageenan-Induced Hyperalgesia. Because ELN-441958 has lower potency at rodent than primate B_1 receptors, it was evaluated in a primate pain model. ELN441958 dose-dependently reduced the thermal hyperalgesia elicited by carrageenan injected into the tail (Fig. 9). In this tail-withdrawal procedure, carrageenan injection (2 mg/tail) produced a thermal hyperalgesia manifested by a reduced tail-withdrawal latency from 20 s (baseline) to 1 to 2 s in 46°C water. A 30-min pretreatment with 10 mg/kg ELN441958 s.c. completely blocked this hyperalgesia after 1 to 1.5 h postcarrageenan injection, and this antihyperalgesic effect was maintained for at least 3.5 h, consistent with sustained pla-

TABLE 7
Pharmacokinetic parameters for ELN441958 in the rat and rhesus monkey
See *Materials and Methods* for description of the assays. Values are presented as means ± S.E.M. from a single study (rat, $n = 3$; rhesus, $n = 3$).

Parameter	Rat	Rhesus
i.v. dose (mg/kg)	2.5	1
i.v. $t_{1/2}$ (h)	2.0 ± 0.8	3.9 ± 0.3
i.v. $AUC_{0\text{-}t}$ (μg · h/ml)	2.6 ± 0.3	2.1 ± 0.3
i.v. Vz (l/kg)	2.7 ± 0.7	2.7 ± 0.4
i.v. clearance (l/h/kg)	0.96 ± 0.12	0.49 ± 0.06
Oral dose (mg/kg)	10	5
Oral C_{max} (μg/ml)	1.3 ± 0.5	4.0 ± 0.1
Oral T_{max} (h)	1.7 ± 0.6	3.3 ± 0.7
Oral $AUC_{0\text{-}t}$ (μg · h/ml)	6.0 ± 1.4	14 ± 0
Oral bioavailability (%)	57	~100[a]
s.c. dose (mg/kg)		10
s.c. C_{max} (μg/ml)		5.6 ± 1.8
s.c. T_{max} (h)		2.2 ± 1.0
s.c. $AUC_{0\text{-}t}$, (μg · h/ml)		27 ± 6
s.c. bioavailability (%)		~100[a]

[a] The oral and s.c. bioavailability of ELN441958 exceeded the maximum possible (100%), and they were calculated to be 138 ± 17 and 137 ± 40%, respectively.

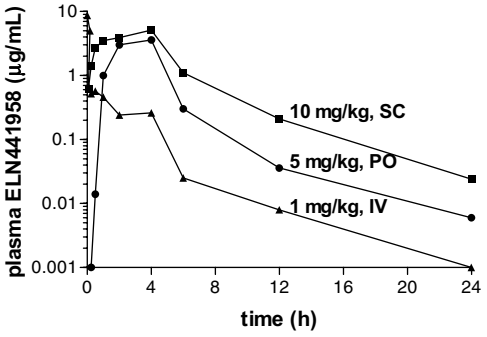

Fig. 8. ELN441958 exhibits a favorable pharmacokinetic profile in the rhesus monkey. Male rhesus monkeys were dosed i.v. at 1 mg/kg in 10% polyethylene glycol 660 hydroxystearate/HCl/saline or orally at 5 mg/kg in 10% polyethylene glycol 660 hydroxystearate/HCl/water or s.c. at 10 mg/kg in 20% Captisol/water ($n = 3$). See *Materials and Methods* for analytical details. Facial flushing was noted in all animals 0 to 3 min following i.v. bolus injection, and in one of three animals 16 min after the s.c. injection.

teau plasma levels up to 4 h following s.c. administration (Fig. 8). At 3 mg/kg, ELN441958 produced a clear antihyperalgesic effect only at times greater than 1.5 h postcarrageenan injection and complete block was achieved in all three subjects by 3.5 h. The large error bars at this dose were the result of different time intervals required to reach baseline by each of the three subjects. Because a dose of 1 mg/kg had no effect on carrageenan-induced hyperalgesia, the minimal effective dose for ELN441958 was 3 mg/kg s.c. in this model. Plasma levels of ELN441958 at the 4-h time point were 0.20 ± 0.06, 1.1 ± 0.26, and 5.0 ± 2.0 μM at the 1, 3, and 10 mg/kg doses, respectively.

ELN441958 produced signs in certain subjects at doses reducing carrageenan-induced hyperalgesia. Facial flushing was observed in two of three monkeys at the 10 mg/kg dose, occurring within 30 min after compound injection. The observed facial flushing may be due to a release of histamine by the compound as elevated plasma histamine levels were detected 1 to 5 min following i.v. administration of 1 mg/kg ELN441958 in rhesus monkeys in the PK study (range 30–160 ng histamine/ml plasma; $n = 3$). This possibility was not explored further in efficacy studies. In addition, facial paling was observed in all three subjects at the 10 mg/kg dose

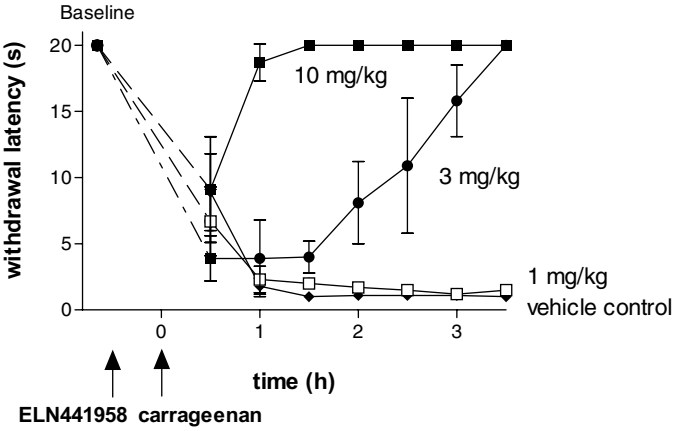

Fig. 9. ELN441958 dose-dependently reduced carrageenan-induced hyperalgesia in rhesus monkeys. ELN441958 or vehicle was injected s.c. 30 min before local injection of carrageenan into the tail. Tail-withdrawal latencies in 46°C water were determined at 30-min intervals following carrageenan injection. Vehicle control data (open squares) partially superimposes on the 1 mg/kg dose (closed diamonds). Each symbol represents the mean ± S.E.M. for three subjects in a single dosing session.

between 0.5 and 2.5 h postcarrageenan injection. Finally, one monkey at 10 mg/kg seemed to be slightly sedated during the entire test session as evidenced by occasional eye closure, although this animal was readily aroused for testing tail-withdrawal latency. The cause of the facial paling and apparent sedation are not known. Although the signs observed at the 10 mg/kg dose are of some concern for the safety of the compound, it is unlikely that they complicated the interpretation of the increase in withdrawal latencies, because they were not observed at the 3 mg/kg dose, which was efficacious in all subjects. In addition, facial flushing had resolved in all subjects before the first tail-withdrawal latency measurement.

To determine whether opioid receptors are involved in the antihyperalgesic effect of ELN441958, the effect of pretreatment with the opioid receptor antagonist naltrexone was determined. Naltrexone (1 mg/kg s.c.) administered just before ELN441958 (10 mg/kg s.c.) had no effect on the reduction of carrageenan-induced hyperalgesia by ELN441958, suggesting that opioid receptors are not involved in this effect (Fig. 10).

Naproxen was selected as a reference nonsteroidal anti-inflammatory drug for comparison with ELN441958. Naproxen (10 mg/kg s.c.) produced a time-dependent reduction in the carrageenan-induced thermal hyperalgesia in rhesus monkeys (Fig. 11). The reduction in hyperalgesia was apparent 2 h postcarrageenan injection, and all subjects reached baseline thresholds by 2.5 to 3 h. Similar antihyperalgesic effects were observed by 10 mg/kg naproxen and 3 mg/kg ELN441958 (Fig. 9). At the identical dose of 10 mg/kg, ELN441958 reduced hyperalgesia from 0.5 to 3.5 h after carrageenan injection, whereas naproxen was only effective at times ≥2 h postcarrageenan, indicating that ELN441958 is more effective than an equivalent dose of naproxen in reducing carrageenan-induced hyperalgesia at early time points.

Discussion

The benzamide ELN441958 is an optimized member of a new class of nonpeptide bradykinin B_1 receptor antagonists.

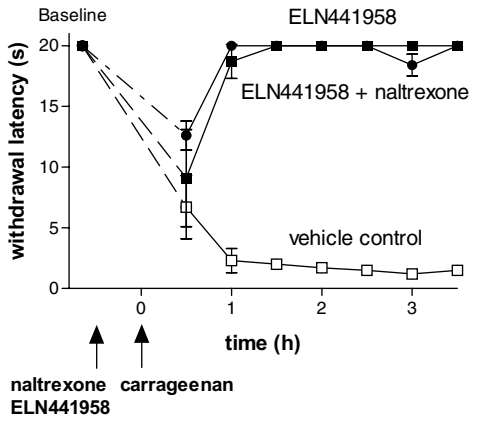

Fig. 10. The opioid-receptor antagonist naltrexone does not affect the antihyperalgesic effect of ELN441958 in the rhesus carrageenan model. Naltrexone (1 mg/kg s.c.) was injected just before ELN441958 (10 mg/kg s.c.). The vehicle control and ELN441958 alone data are the same as in Fig. 9. Each symbol represents the mean ± S.E.M. for three subjects in a single dosing session.

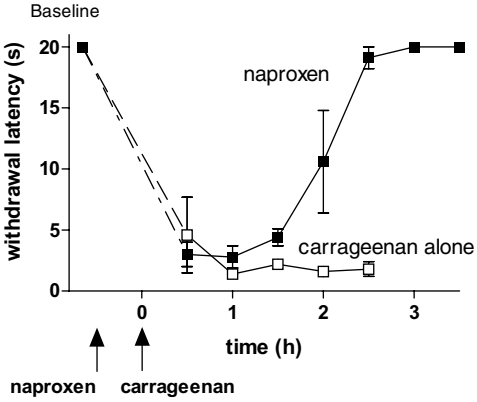

Fig. 11. Naproxen reduces carrageenan-induced hyperalgesia in rhesus monkeys. Naproxen (10 mg/kg s.c.) was injected 30 min before local injection of carrageenan into the tail. See Fig. 9 and *Materials and Methods* for details. Each symbol represents the mean ± S.E.M. for three individuals in a single dosing session.

The benzamide core was predicted to confer activity based on molecular modeling studies involving the crystal structure of a series of potent B_1 receptor antagonists, the 3,4-dihydroquinoxalinones (Grant et al., 2006). This modeling suggested that the quinoxalinone core and its substituents could be effectively replaced by a substituted benzamide, and initial compounds synthesized proved to be low micromolar B_1 antagonists. Modifications designed to increase structural rigidity resulted in increased activity and also improved oral bioavailability, ultimately leading to ELN441958.

ELN441958 is a potent, selective, neutral antagonist of the human bradykinin B_1 receptor. It has subnanomolar affinity for displacement of the agonist ligand [^{3}H]DAKD. In saturation binding studies, ELN441958 reduced the apparent affinity of [^{3}H]DAKD more than 4-fold with little change in measured receptor density, consistent with reversible, competitive displacement of the agonist radioligand from the human B_1 receptor. Other types of small molecule antagonists whose mode of binding has been investigated have also been shown to compete with agonist, including the sulfonamide SSR240612 (Gougat et al., 2004), the quinoxaline compound A (Ransom et al., 2004), and the *N*-methylacetamide LF22-0542 (Porreca et al., 2006). ELN441958 is also a subnanomolar antagonist of agonist (DAKD)-induced calcium mobilization in IMR-90 cells expressing the native human B_1 receptor. No agonist-like activity was detected by ELN-441958 alone in calcium mobilization studies, indicating that ELN441958 is a neutral antagonist of the B_1 receptor. In the same cells, ELN441958 does not inhibit the activation of the human bradykinin B_2 receptor at concentrations up to 10 μM, showing that it is highly selective for B_1 over B_2 receptors. ELN441958 also displays good selectivity for B_1 over other receptors examined in a broad screening panel. It is >500-fold selective for the B_1 receptor over the human μ-opioid receptor, the most potent off-target activity identified.

ELN441958 has marked species differences for B_1 receptor antagonist potency compared with the peptidic B_1 receptor antagonists DALKD and *des*Arg^{10}HOE140. Agonist-induced calcium mobilization experiments indicate that ELN441958 is 120-fold less potent at the mouse B_1 receptor relative to the human receptor. Similar species differences have been noted previously for other series of small molecule B_1 receptor antagonists, including the quinoxalines and the diaminopyridines (Kuduk et al., 2004; Ransom et al., 2004). These findings are consistent with the relatively low sequence homology between B_1 receptors from human and mouse (72%; Hess et al., 1996) or rat (73%; Jones et al., 1999). Because there is high sequence homology between the mouse and rat receptor (90%; Jones et al., 1999), it is surprising that ELN441958 is 10-fold more potent at the rat than mouse B_1 receptor. Of residues known to be involved in the binding of peptides or small molecule ligands (Ha et al., 2005), only Ile97 in the human sequence shows divergence between the corresponding locations in the rat (Ile107) and mouse (Val104) sequences. Site-directed mutagenesis studies would be required to determine whether this conserved substitution can account for the species differences observed.

MDCK-MDR1 permeability and ATPase assays indicate that ELN441958 is a substrate for human P-gp. Consistent with these in vitro results, ELN441958 had low CNS penetration in the mouse. Antagonism of spinal B_1 receptors may be important to achieve full analgesic efficacy of an orally delivered antagonist as suggested by the efficacy of intrathecally delivered B_1 receptor antagonists in pain models (Fox et al., 2003; Conley et al., 2005). Alternatively, it is possible that brain penetration may lead to increased central side effects, because there is a high level of constitutive B_1 receptor expression in monkey brains (Shughrue et al., 2003), and the B_1 receptor is expressed in human brain (Raidoo and Bhoola, 1997). Nevertheless, peripherally acting peptidic B_1 receptor antagonists given systemically are effective in pain models. For example, *des*Arg^{10}HOE140 is effective against CFA-induced mechanical allodynia by either the intrathecal or s.c. route (Fox et al., 2003). An antagonist that is excluded from the spinal cord could still block B_1 receptors present on peripheral terminals of sensory fibers, and it may also gain access to receptors present on cell bodies in the dorsal root ganglion (DRG).

ELN441958 possesses a favorable pharmacokinetic profile as predicted by in vitro assays. ELN441958 is well absorbed after oral administration in rats and rhesus monkeys consistent with the moderate solubility and permeability in MDCK cells. In particular, ELN441958 is essentially completely absorbed and produces high plasma levels after oral adminis-

tration in rhesus monkeys. The bioavailabilities calculated following oral and s.c. administration in monkeys were greater than 100%, possibly due to lack of dose proportionality by one or more route of administration as different dose levels used for each route. ELN441958 has a moderate clearance and volume of distribution in both species following i.v. administration, consistent with the high metabolic stability in rat, rhesus, and human microsomes. The high oral bioavailability and half-life of ~4 h in rhesus monkeys coupled with the good metabolic stability in human microsomes predict a favorable pharmacokinetic profile for ELN441958 in humans.

Several approaches have been taken to demonstrate efficacy for B_1 antagonists with low potency at rodent B_1 receptors, precluding their evaluation in standard rodent pain models. For example, Su et al. (2003) exploited the pharmacological similarity between primate and rabbit B_1 receptors by demonstrating the potent efficacy of a quinoxaline B_1 receptor antagonist in a CFA-induced hyperalgesia in rabbits. In an elegant study by Fox et al. (2005), the highly human-selective B_1 receptor antagonist NVP-SAA164 reversed CFA-induced hyperalgesia in transgenic mice expressing only the human B_1 receptor. An alternative approach is to evaluate compounds in primate pain models.

Use of primate pain and inflammation models to evaluate potential therapeutic agents is advantageous for several reasons. In addition to species differences in receptor potency, a clear advantage of the use of primate models is the more direct applicability to humans. There are often major differences in the pharmacology of neurotransmitter systems involved in pain transmission between humans and rodents, e.g., cholecystokinin (Hökfelt et al., 2001) and substance P (Hill, 2000). In addition, scaling from monkey pharmacokinetic data is generally the most accurate method to predict human clearance (Evans et al., 2006). In the bradykinin system, human and monkey B_1 receptors are functionally indistinguishable, whereas rodent receptors exhibit a different agonist and antagonist pharmacology (Regoli et al., 2001). Demonstration of efficacy in primates using experimental analgesic agents with novel mechanisms of action not validated clinically increases the likelihood of analgesic efficacy in humans.

The rhesus monkey tail-withdrawal procedure is a well characterized method for assessing antinociception in primates. Initially established as an acute pain model, the procedure involves measuring the latency to withdrawal of the tail immersed in water at an acutely noxious temperature (e.g., 50°C) (Ko et al., 2004). Trained monkeys respond to standard analgesic agents such as opioids with an increased latency to tail withdrawal. To evaluate analgesics with a broader range of mechanisms, the procedure has been modified by pretreatment with agents that sensitize the tail to thermal stimuli. For example, topical application of capsaicin produces a gradual and relatively prolonged hyperalgesia, and it closely mimics the experimental use of capsaicin in humans (Butelman et al., 2003). Alternatively, carrageenan injection into the tail of rhesus monkeys produces a thermal hyperalgesia manifested as a reduced tail-withdrawal latency to a normally non-noxious water temperature (Ko and Lee, 2002). The latency to withdrawal in 46°C water is reduced to 1 to 2 s from a baseline of 20 s within 1 h after carrageenan injection and is maintained for at least 3.5 h.

ELN441958 dose-dependently reduces carrageenan-induced thermal hyperalgesia in rhesus monkeys, with a minimal effective dose of 3 mg/kg s.c. At this dose, ELN441958 does not affect the initial hyperalgesia produced by carrageenan, but it reduces hyperalgesia beginning 2 h after carrageenan injection, and it completely blocks the hyperalgesia by 3.5 h postinjection. The delayed antihyperalgesic effect observed at 3 mg/kg ELN441958 s.c. may be due to a progression of inflammatory mediators producing hyperalgesia following carrageenan injection. Specifically, generation of prostanoids may play a dominant role in carrageenan-induced hyperalgesia after about 2 h postcarrageenan injection, but not earlier. This idea is supported by a similar time-dependent reduction in hyperalgesia observed with the nonselective cyclooxygenase inhibitor naproxen at 10 mg/kg s.c., which probably reflects the time course for prostanoid production caused by carrageenan. The time-dependent reduction in carrageenan hyperalgesia observed at the 3 mg/kg dose of ELN441958 probably represents antagonism of B_1 receptor-mediated prostanoid production.

The early carrageenan-induced hyperalgesia may be unrelated to prostanoid production, and it is thus not sensitive to treatment with 10 mg/kg naproxen s.c. It has been shown that during the first hour following carrageenan injection into the rat paw, edema develops that is mediated by histamine, serotonin, and bradykinin release (Salvemini et al., 1996). Subsequently, neutrophil infiltration and production of NO, tumor necrosis factor-α, interferon-γ, cytokines (IL-1 and IL-2), and prostaglandins contribute significantly to the edema 1 to 6 h after carrageenan injection. In particular, NO production has been shown to dramatically increase within 1 h, whereas prostaglandin E_2 levels increase slowly, peaking at 3 h after carrageenan injection (Salvemini et al., 1996). Thus, it is likely that the high dose of 10 mg/kg ELN441958 s.c. reduces early carrageenan-induced hyperalgesia by mechanisms other than prostanoid production. Because B_1 agonists promote generation of NO (Sangsree et al., 2003), cytokine release (Tsukagoshi et al., 1999), and neutrophil infiltration (Ehrenfeld et al., 2006), B_1 antagonists may reduce the hyperalgesia elicited by these proinflammatory factors.

The potential contribution of receptor induction to the antihyperalgesic effects of ELN441958 in the carrageenan model must be considered. The peripheral non-neuronal effects of B_1 antagonists require receptor induction as receptor expression is normally very low or nondetectable. B_1 receptor induction in peripheral tissues can occur rapidly following tissue insult. For example, B_1 receptor mRNA is dramatically increased in the paw within 1 h following paw injection of IL-1β (Campos et al., 2002). Carrageenan paw injection increases B_1 mRNA paw expression at 3 h in rats (J. E. Hawkinson, unpublished observations). Taken together, these data suggest that carrageenan injection may rapidly (i.e., within about 1 h) induce B_1 receptors in peripheral tissues. In contrast to non-neural tissues, constitutive expression of the B_1 receptor in nociceptors has been demonstrated (Wotherspoon and Winter, 2000). Paw injection of CFA results in up-regulation of B_1 receptor in the DRG after 24 h (Fox et al., 2003). Efficacy of 3 mg/kg ELN441958 in rhesus monkeys observed at times later than 1 h postcarrageenan injection are consistent with the time course for local B_1 receptor induction, again suggesting a peripheral action at this dose.

Rapid effects of 10 mg/kg ELN441958 observed within 1 h after carrageenan injection may require blockade of constitutive B_1 receptors expressed on pain afferents. Consistent with this idea, ELN441958 (3 and 10 mg/kg s.c.) produced a marked reduction in topically applied capsaicin-induced allodynia in rhesus monkeys within 5 min after removal of capsaicin. Antiallodynic activity of ELN441958 was observed in two of the four rhesus monkeys tested in a tail-withdrawal procedure using both 38 and 42°C stimulation (E. R. Butelman, unpublished observations). Because ELN441958 has poor penetration into the spinal cord, the antihyperalgesic activity at low doses is more likely mediated by B_1 receptors expressed on nociceptors at their peripheral terminals or at the cell bodies in the DRG, although high doses may be sufficient to penetrate the spinal cord and exert a central antihyperalgesic effect. Intrathecally administered B_1 receptor antagonists are effective in acute and inflammatory pain models (Fox et al., 2003; Conley et al., 2005).

Plasma levels achieved by ELN441958 at efficacious doses were substantially greater than its in vitro potency. This difference may be explained by a number of factors related to the compound and/or the receptor. For example, ELN441958 has restricted access to neuronal B_1 receptors expressed in spinal cord and access to receptors expressed on cell bodies in the DRG may also be limited. Accessibility to peripheral B_1 receptors may also be restricted if the compound is highly bound to plasma proteins. In addition, time-dependent upregulation of B_1 receptor expression and the progression of inflammatory mediators with varying sensitivities to modulation by B_1 receptor antagonism following carrageenan injection may also contribute to the relatively high doses of ELN441958 required for efficacy.

Because ELN441958 has low affinity for μ- and δ-opioid receptors (i.e., it is >500- and >2000-fold selective for the human B_1 receptor over μ- and δ-opioid receptors, respectively), opioid receptors may play a minimal role in its antihyperalgesic effects. This notion is further supported by the finding that naltrexone 1 mg/kg s.c. was inactive in blocking the antihyperalgesic effects of ELN441958. Based on the binding affinity of naltrexone in monkey brain membranes and its in vivo antagonist potency in rhesus monkeys (Emmerson et al., 1994; Ko et al., 1998), this dose of naltrexone is sufficient to antagonize μ-, κ-, or δ-opioid receptor-mediated behavioral effects in monkeys. Although in this study we did not conduct a control experiment to show blockade of opioid receptor-mediated effects by this dose of naltrexone, several studies have shown that much smaller doses (i.e., 0.0032–0.1 mg/kg) antagonized a variety of opioid-mediated behavioral effects in rhesus monkeys (Ko et al., 1998, 2004; Bowen et al., 2002). For example, naltrexone 0.1 mg/kg produced a 10-fold rightward shift of the dose-response curve for μ-opioid agonist-induced antinociception (Ko et al., 1998). Taken together, it is unlikely that the opioid receptors significantly contribute to the antihyperalgesic effects of ELN441958 in monkeys.

In summary, ELN441958 is an optimized lead compound of a novel class of bradykinin B_1 receptor antagonists. ELN441958 is a potent, competitive, neutral antagonist of the human B_1 receptor, with lower potency at rodent B_1 receptors. It has a favorable pharmacokinetic profile in rats and rhesus monkeys as predicted by in vitro metabolism and permeability assays. ELN441958 is a P-gp substrate, consistent with low CNS exposure. ELN441958 reduced carrageenan-induced hyperalgesia in rhesus monkeys, probably acting primarily at peripheral B_1 receptors. Validation of the therapeutic utility of bradykinin B_1 antagonists in the treatment of human pain states will require evaluation in clinical trials.

Acknowledgments

We thank Dr. Barbara Jagodzinska (Elan Pharmaceuticals) for the synthesis of indinavir.

References

Bowen CA, Fischer BD, Mello NY, and Negus SS (2002) Antagonism of the antinociceptive and discriminative stimulus effects of heroin and morphine by 3-methoxynaltrexone and naltrexone in rhesus monkeys. *J Pharmacol Exp Ther* **302:** 264–273.

Butelman ER, Ball JW, Harris TJ, and Kreek MJ (2003) Topical capsaicin-induced hyperalgesia in unanesthetized primates: pharmacological modulation. *J Pharmacol Exp Ther* **306:**1106–1114.

Campos MM, de Souza GE, Ricci ND, Pesquero JL, Teixeira MM, and Calixto JB (2002) The role of migrating leukocytes in IL-1β-induced up-regulation of kinin B_1 receptors in rats. *Br J Pharmacol* **135:**1107–1114.

Conley RK, Wheeldon A, Webb JK, DiPardo RM, Homnick CF, Bock MG, Chen TB, Chang RS, Pettibone DJ, and Boyce S (2005) Inhibition of acute nociceptive responses in rat spinal cord by a bradykinin B_1 receptor antagonist. *Eur J Pharmacol* **527:**44–51.

Demeule M, Regina A, Jodoin J, Laplante A, Dagenais C, Berthelet F, Moghrabi A, and Beliveau R (2002) Drug transport to the brain: key roles for the efflux pump P-glycoprotein in the blood-brain barrier. *Vascul Pharmacol* **38:**339–348.

Eisenbarth H, Rukwied R, Petersen M, and Schmelz M (2004) Sensitization to bradykinin B1 and B2 receptor activation in UV-B irradiated human skin. *Pain* **110:**197–204.

Ehrenfeld P, Millan C, Matus CE, Figueroa JE, Burgos RA, Nualart F, Bhoola KD, and Figueroa CD (2006) Activation of kinin B_1 receptors induces chemotaxis of human neutrophils. *J Leukoc Biol* **80:**117–124.

Emmerson PL, Liu MR, Woods JH, and Medzihradsky F (1994) Binding affinity and selectivity of opioids at *mu*, *delta* and *kappa* receptors in monkey brain membranes. *J Pharmacol Exp Ther* **271:**1630–1637.

Evans CA, Jolivette LJ, Nagilla R, and Ward KW (2006) Extrapolation of preclinical pharmacokinetics and molecular feature analysis of "discovery-like" molecules to predict human pharmacokinetics. *Drug Metab Dispos* **34:**1255–1265.

Ferreira J, Campos MM, Araujo R, Bader M, Pesquero JB, and Calixto JB (2002) The use of kinin B_1 and B_2 receptor knockout mice and selective antagonists to characterize the nociceptive responses caused by kinins at the spinal level. *Neuropharmacology* **43:**1188–1197.

Ferreira J, Campos MM, Pesquero JB, Araujo RC, Bader M, and Calixto JB (2001) Evidence for the participation of kinins in Freund's adjuvant-induced inflammatory and nociceptive responses in kinin B_1 and B_2 receptor knockout mice. *Neuropharmacology* **41:**1006–1012.

Fox A, Kaur S, Li B, Panesar M, Saha U, Davis C, Dragoni I, Colley S, Ritchie T, Bevan S, et al. (2005) Antihyperalgesic activity of a novel nonpeptide bradykinin B_1 receptor antagonist in transgenic mice expressing the human B_1 receptor. *Br J Pharmacol* **144:**889–899.

Fox A, Wotherspoon G, McNair K, Hudson L, Patel S, Gentry C, and Winter J (2003) Regulation and function of spinal and peripheral neuronal B_1 bradykinin receptors in inflammatory mechanical hyperalgesia. *Pain* **104:**683–691.

Gougat J, Ferrari B, Sarran L, Planchenault C, Poncelet M, Maruani J, Alonso R, Cudennec A, Croci T, Guagnini F, et al. (2004) SSR240612 [(2*R*)-2-[((3*R*)-3-(1,3-Benzodioxol-5-yl)-3-[[(6-methoxy-2-naphthyl)sulfonyl]amino]propanoyl)amino]-3-(4-[[2*R*,6*S*)-2,6-dimethylpiperidinyl]methyl]phenyl)-*N*-isopropyl-*N*-methylpropanamide hydrochloride], a new nonpeptide antagonist of the bradykinin B_1 receptor: biochemical and pharmacological characterization. *J Pharmacol Exp Ther* **309:**661–669.

Grant FS, Bartulis S, Brogley L, Dappen MS, Kasar R, Holcomb R, Pleiss MA, Thorsett ED, Ye M, and Hawkinson JE (2006) inventors; Elan Pharmaceuticals, Inc., assignee. Sulfonylquinoxaline derivatives as bradykinin antagonists. U.S. Patent 7,056,937. 2006 Jun 6.

Ha SN, Hey PJ, Ransom RW, Bock MG, Su DS, Murphy KL, Chang R, Chen TB, Pettibone D, and Hess JF (2006) Identification of the critical residues of bradykinin receptor B1 for interaction with the kinins guided by site-directed mutagenesis and molecular modeling. *Biochemistry* **45:**14355–14361.

Hess JF, Derrick AW, MacNeil T, and Borkowski JA (1996) The agonist selectivity of a mouse B1 bradykinin receptor differs from human and rabbit B1 receptors. *Immunopharmacology* **33:**1–8.

Hill R (2000) NK_1 (substance P) receptor antagonists- why are they not analgesic in humans. *Trends Pharmacol Sci* **21:**244–246.

Hökfelt T, Holmberg K, Shi TJ, and Broberger C (2001) CCK-ergic mechanisms in sensory systems. *Scand J Clin Lab Invest Suppl* **234:**69–74.

Jones C, Phillips E, Davis C, Arbuckle J, Yaqoob M, Burgess GM, Docherty RJ, Webb M, Bevan SJ, and McIntyre P (1999) Molecular characterisation of cloned bradykinin B_1 receptors from rat and human. *Eur J Pharmacol* **374:**423–433.

Ko MC, Butelman ER, Traynor JR, and Woods JH (1998) Differentiation of *kappa* opioid agonist-induced antinociception by naltrexone apparent pA_2 analysis in rhesus monkeys. *J Pharmacol Exp Ther* **285:**518–526.

Ko MC and Lee H (2002) An experimental model of inflammatory pain in monkeys:

comparison of antinociceptive effects of opioids and NSAIDs against carrageenan-induced thermal hyperalgesia, in *10th World Congress on Pain (Abstract)*, p. 136, International Association for the Study of Pain (IASP) Press, Seattle, WA.

Ko MCH, Song MS, Edwards T, Lee H, and Naughton NN (2004) The role of central mu opioid receptors in opioid-induced itch in primates. *J Pharmacol Exp Ther* **310:**169–176.

Kuduk SD, Ng C, Feng DM, Wai JM, Chang RS, Harrell CM, Murphy KL, Ransom RW, Reiss D, Ivarsson M, et al. (2004) 2,3-Diaminopyridine bradykinin B_1 receptor antagonists. *J Med Chem* **47:**6439–6442.

Lawson SR, Gabra BH, Nantel F, Battistini B, and Sirois P (2005) Effects of a selective bradykinin B_1 receptor antagonist on increased plasma extravasation in streptozotocin-induced diabetic rats: distinct vasculopathic profile of major key organs. *Eur J Pharmacol* **514:**69–78.

Leeb-Lundberg LM, Marceau F, Muller-Esterl W, Pettibone DJ, and Zuraw BL (2005) International union of pharmacology. XLV. Classification of the kinin receptor family: from molecular mechanisms to pathophysiological consequences. *Pharmacol Rev* **57:**27–77.

Levy D and Zochodne DW (2000) Increased mRNA expression of the B1 and B2 bradykinin receptors and antinociceptive effects of their antagonists in an animal model of neuropathic pain. *Pain* **86:**265–271.

MacNeil T, Feighner S, Hreniuk DL, Hess JF, and Van der Ploeg LH (1997) Partial agonists and full antagonists at the human and murine bradykinin B_1 receptors. *Can J Physiol Pharmacol* **75:**735–740.

McLean PG, Ahluwalia A, and Perretti M (2000) Association between kinin B_1 receptor expression and leukocyte trafficking across mouse mesenteric postcapillary venules. *J Exp Med* **192:**367–380.

Meini S, Lecci A, and Maggi CA (1996) The longitudinal muscle of rat ileum as a sensitive monoreceptor assay for bradykinin B_1 receptors. *Br J Pharmacol* **117:**1619–1624.

Perkins MN, Campbell E, and Dray A (1993) Antinociceptive activity of the bradykinin B1 and B2 receptor antagonists, des-Arg^9, [Leu^8]-BK and HOE 140, in two models of persistent hyperalgesia in the rat. *Pain* **53:**191–197.

Pesquero JB, Araujo RC, Heppenstall PA, Stucky CL, Silva JA, Walther T, Oliveira SM, Pesquero JL, Paiva AC, Calixto JB, et al. (2000) Hypoalgesia and altered inflammatory responses in mice lacking kinin B1 receptors. *Proc Natl Acad Sci U S A* **97:**8140–8145.

Poole S, Lorenzetti BB, Cunha JM, Cunha FQ, and Ferreira SH (1999) Bradykinin B_1 and B_2 receptors, tumour necrosis factor α and inflammatory hyperalgesia. *Br J Pharmacol* **126:**649–656.

Porreca F, Vanderah TW, Guo W, Barth M, Dodey P, Peyrou V, Luccarini JM, Junien JL, and Pruneau D (2006) Antinociceptive pharmacology of *N*-[[4-(4,5-dihydro-1*H*-imidazol-2-yl)phenyl]methyl]-2-[2-[[(4-methoxy-2,6-dimethylphenyl) sulfonyl]-methylamino]ethoxy]-*N*-methylacetamide, fumarate (LF22-0542), a novel nonpeptidic bradykinin B_1 receptor antagonist. *J Pharmacol Exp Ther* **318:**195–205.

Raidoo DM and Bhoola KD (1997) Kinin receptors on human neurones. *J Neuroimmunol* **77:**39–44.

Ransom RW, Harrell CM, Reiss DR, Murphy KL, Chang RS, Hess JF, Miller PJ, O'Malley SS, Hey PJ, Kunapuli P, et al. (2004) Pharmacological characterization and radioligand binding properties of a high-affinity, nonpeptide, bradykinin B_1 receptor antagonist. *Eur J Pharmacol* **499:**77–84.

Regoli D, Rizzi A, Perron SI, and Gobeil F (2001) Classification of kinin receptors. *Biol Chem* **382:**31–35.

Salvemini D, Wang ZQ, Wyatt PS, Bourdon DM, Marino MH, Manning PT, and Currie MG (1996) Nitric oxide: a key mediator in the early and late phase of carrageenan-induced rat paw inflammation. *Br J Pharmacol* **118:**829–838.

Sangsree S, Brovkovych V, Minshall RD, and Skidgel RA (2003) Kininase I-type carboxypeptidases enhance nitric oxide production in endothelial cells by generating bradykinin B_1 receptor agonists. *Am J Physiol* **284:**H1959–H1968.

Shughrue PJ, Ky B, and Austin CP (2003) Localization of B1 bradykinin receptor mRNA in the primate brain and spinal cord: an in situ hybridization study. *J Comp Neurol* **465:**372–384.

Su DS, Markowitz MK, DiPardo RM, Murphy KL, Harrell CM, O'Malley SS, Ransom RW, Chang RS, Ha S, Hess FJ, et al. (2003) Discovery of a potent, non-peptide bradykinin B_1 receptor antagonist. *J Am Chem Soc* **125:**7516–7517.

Tsukagoshi H, Shimizu Y, Horie T, Fukabori Y, Shimizu Y, Iwamae S, Hisada T, Ishizuka T, Iizuka K, Dobashi K, et al. (1999) Regulation by interleukin-1β of gene expression of bradykinin B_1 receptor in MH-S murine alveolar macrophage cell line. *Biochem Biophys Res Commun* **259:**476–482.

Wotherspoon G and Winter J (2000) Bradykinin B1 receptor is constitutively expressed in the rat sensory nervous system. *Neurosci Lett* **294:**175–178.

Address correspondence to: Dr. Jon E. Hawkinson, Lead Discovery and Optimization, Elan Pharmaceuticals, 800 Gateway Blvd., South San Francisco, CA 94080. E-mail: jon.hawkinson@earthlink.net